

# Comparative Study of Different Control Strategies in Permanent Magnet Synchronous Motor Drives

Vishesh Biyani, Jinesh R, Tharani Eswar T A, Sithartha Sourya V S and Pinkymol K.P

*Department of Electrical and Electronics Engineering*

*National Institute of Technology Tiruchirappalli, Tamil Nadu 620015, India*

{visheshlm10, jineshrs2398, guruesvar1299, sitharthasourya98}@gmail.com, pinkymol@ieee.org

**Abstract**—The main goal of this paper is to evaluate and compare various control schemes (scalar control vs vector control) in Permanent Magnet Synchronous Motor (PMSM). Mathematical modelling of PMSM was implemented and used for this paper. Under scalar control, the V/f method is studied. Under vector control, Field Oriented Control (FOC), Direct Torque Control (DTC), Direct Torque Control with Space Vector Modulation (DTC-SVM) are extensively studied. By using MATLAB/Simulink, these control algorithms are implemented in a PMSM motor drive. To that end, MATLAB/Simulink simulations were used to examine and compare the control output of Scalar, FOC, and DTC from various perspectives. Further, it is shown that the shortcomings of the classical DTC control technique are resolved by DTC-SVM control to get a satisfactory control with computational demand as the trade-off. This study compares these control schemes based on the parameters of an existing 2.135-kW surface mounted non-salient sinusoidal flux distribution PMSM to find the noteworthy features associated with each control scheme to understand which control method is to be preferred where and for what desired accuracy.

**Keywords:** PMSMs, DTC, FOC, DTC-SVM, VFDs, PWM

## I. INTRODUCTION

Motor control systems are critical in the new advanced modern industry and society. It has various applications, from general-purpose variable-speed drives like wind turbines to high-performance robots, CNC devices, and electric cars. In recent years, due to development in power electronics and modern control theory, the development of AC motor drives became convenient. PMSMs are gaining a significant share of the EV motor drive market. Because of its popularity, an increasing number of researchers are focusing on improved control techniques for PMSM drives, which significantly improve dynamic efficiency, device resilience and reduce the complexity of PMSM drive control systems. I.boldea, a. Moldovan and Tutelea [1] presents an overview of scalar control (V/f and I-f) with open and closed-loop stabilization for wide-range speed control of induction and synchronous motor drives.[2], [3] Describes about the implementation and modelling of Direct Torque Control (DTC) in PMSM drives respectively. A thorough investigation has been carried out in [4], and [5] which gives a brief simulation study and the implementation of DTC using SVPWM control strategy (DTC-SVM). In E. Yesilbag and L. T. Ergene [6] discuss the configuration and simulation of the field-oriented control (FOC) of the synchronous permanent magnet motor, which

is one of the most often used industrial control systems. Turksoy, Omer & Yilmaz, Unal & Tan and Adnan Teke, in Ahmet. [7] presents the comparison of DTC and FOC control strategies. [8] Discusses the techniques used to control voltage source inverters in modulated pulse width waves. Some of the most efficient approaches discussed are modulation of sinusoidal pulse width and modulation techniques of space vector pulse width.

In this paper, we compare and evaluate the control strategies present in scalar and vector control. Section II explains the modelling of PMSM. Section III, IV, V, VI demonstrates the theoretical understanding of scalar, FOC, DTC and DTC-SVM control, respectively. Section VII gives a detailed simulation analysis and comparison between each control scheme. Concluding remarks and future scope are mentioned in section VIII.

## II. MODELLING OF PMSM

AC machines have a mathematical model that is time-variant, multi-variable and nonlinear. To achieve a good control of PMSMs, a mathematical model based on the hypothesis below must be developed[9]:

- 1) Core saturation is ignored, regardless of hysteresis loss and core eddy current;
- 2) Permanent magnet material has no electric conductivity;
- 3) The rotor has no damper windings;
- 4) Both the permanent magnet's magnetic field excitation and the three-phase winding's armature reaction are sinusoidally dispersed throughout the air gap.

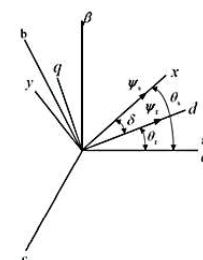


Fig. 1. The flux linkage between stator and the rotor in various reference frames Source: [9]

Fig.1 depicts the relationship between different reference

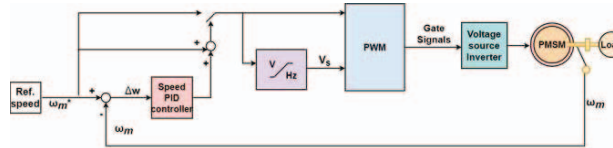


Fig. 2. Block diagram of Scalar Control of PMSM

frames, with  $\psi_s$  denoting the stator flux linkage vector and  $\psi_r$  denoting the rotor (magnet) flux linkage vector. When the stator resistance is ignored, the load angle is formed by the flux linkages between the stator and rotor. The load angle ( $\delta$ ) is constant in the steady-state, corresponding to the load torque, and both the rotor and stator flux rotate at synchronous speeds[10]. The load angle changes during transient operation, and the rotor and stator flux rotate at various speeds. In the dq reference frame, the dynamic equations of the three-phase PMSM are stated as follows[9]:

$$u_{sd} = R_s i_{sd} + \frac{d\psi_{sd}}{dt} - \omega_e \psi_{sq} \quad (1)$$

$$u_{sq} = R_s i_{sq} + \frac{d\psi_{sq}}{dt} + \omega_e \psi_{sd} \quad (2)$$

$$\psi_{sd} = L_d i_{sd} + \psi_f \quad (3)$$

$$\psi_{sq} = L_q i_{sq} \quad (4)$$

$$T_e = \frac{3}{2} * P * (\psi_{sd} i_{sq} - \psi_{sq} i_{sd}) \quad (5)$$

Where  $u_{sd}$ ,  $u_{sq}$ ,  $i_{sd}$ ,  $i_{sq}$ ,  $\psi_{sd}$ ,  $\psi_{sq}$  are respectively d-axis and q-axis stator voltage, current and motor flux in dq reference frame.  $R_s$  represents stator winding resistance,  $\omega_e$  represents electrical angular speed of the rotor and  $T_e$  represents electromagnetic torque.

$$T_e = \frac{3}{2} * P * (\psi_f i_{sq} + (L_d - L_q) i_{sq} i_{sd}) \quad (6)$$

$$\omega_e = P * \omega_m \quad (7)$$

$$J \frac{d\omega_m}{dt} = T_e - T_l - B\omega_m \quad (8)$$

Where  $P$  is the number of pole pairs,  $\psi_f$  is the flux linkage generated by the Permanent Magnets  $L_q$  and  $L_d$  are the q-axis and d-axis inductances of the PMSM. In terms of load angle and stator flux, the equation(6) may also be rewritten, which is:

$$T_e = \frac{3P}{4L_d L_q} |\psi_s| [2\psi_f L_q \sin \delta - |\psi_s| (L_d - L_q) \sin 2\delta] \quad (9)$$

There are two types of electromagnetic torque. The first one is reluctance torque, and the second one is excitation torque this is provided by the permanent magnet flux. The disparity between the asymmetric flux paths in q-axis and d-axis induces reluctance torque in the PMSM with saliency

( $L_d \neq L_q$ ), which is absent in a non-salient pole PMSM[9]. Therefore to avoid disparity of asymmetrical flux in the PMSM, control techniques comparison is made for non-salient or surface mounted pole PMSM as our subject for this paper.

### III. SCALAR CONTROL

In general-purpose industrial AC motor drives, scalar control, also known as V/f control, is common. Fig.2 shows the block diagram of a scalar control scheme in a PMSM drive. The magnitude of stator voltage is adjusted depending on the frequency of operation to regulate the speed of PMSM in V/f control. The drive system's transient behaviour will not be fulfilled because the scalar control focuses mainly on the steady-state dynamics[9]. In this paper, for scalar control, both open loop and closed loop analyses are performed. And in the PWM block, two types of PWM methods are implemented: Sine PWM (SPWM) and Space Vector PWM (SVPWM).

In SPWM, sine wave and triangular wave are compared. The triangular carrier wave and the reference modulating sine wave intersection yields the switching points. SVPWM is achieved by properly selecting inverter switching states and calculating acceptable switching periods. The maximum voltage in SPWM is  $0.5V_{DC}$  but maximum voltage in SVPWM can reach  $0.577V_{DC}$  for amplitude modulation index( $m$ ) = 1. This implies that space vector PWM produces about 15 % higher output voltage than sine PWM. SVPWM technique has a lot of advantages, such as less total harmonic distortion, high output quality. It provides more flexibility in control of output voltage and frequency, the biggest need in AC drives.

### IV. FIELD ORIENTED CONTROL (FOC)

Using Park transformation, the current components corresponding to the field magnetising flux and torque production in AC machines may be separated orthogonally, allowing the field-magnetizing flux to be regulated without disturbing the torque's dynamic behavior and vice versa.[9]. This is the FOC's fundamental principle. Fig.3 shows the block diagram of a PMSM drive mechanism with a FOC control system. FOC control system is divided into two main loops: the d loop, which controls the flux, and the q loop, which controls the torque. The d loop controls the  $i_d$  using a current PID controller. The reference value for the d loop is set to 0. The torque is controlled by the q loop by controlling  $i_q$  using the current PID controller. The speed is controlled using the speed PID controller. The output value of the speed PID controller is given as a reference to the q loop.

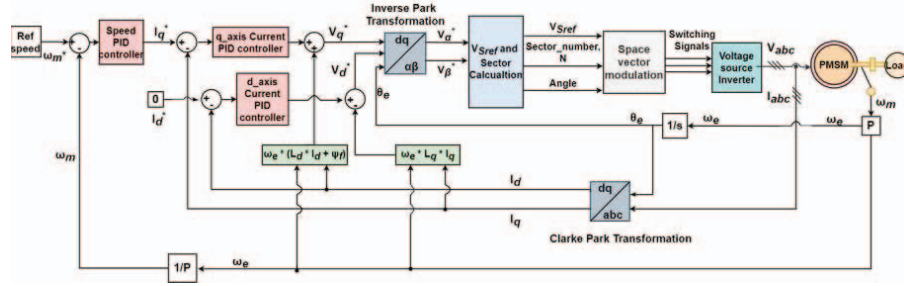


Fig. 3. Block diagram of Field Oriented Control of PMSM

## V. DIRECT TORQUE CONTROL (DTC)

Fig.7 shows the block diagram of the PMSM drive mechanism with the DTC control system. The torque can be regulated quickly with DTC. The amplitude of torque is dependent on the load angle and stator flux linkage as shown by (10) with constant motor parameters in a non-salient pole PMSM ( $L_d = L_q$ )

$$T_e = \frac{3P}{2L_s} |\psi_s| \psi_f \sin \delta \quad (10)$$

Equation (10) implies that the torque increases with increase in  $\delta$ . The regulation of the load torque and stator flux linkage can be accomplished by choosing the necessary stator voltage vectors[10], as shown in the equations and discussions. PMSM drive systems generally operate with three-phase voltage source inverter. The level of the three power switches, which are labelled Sa, Sb, and Sc here, determines the primary voltage Va, Vb, and Vc, as shown in Fig.4

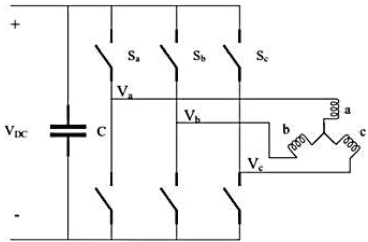
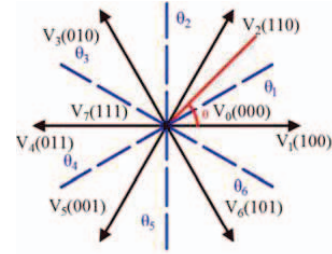


Fig. 4. The voltage source inverter fed PMSM drive system

The controller produces eight voltage space vectors due to the various switching statuses, six of which are non-zero voltage vectors and the rest of which are zero voltage vectors. Each voltage space vector is labelled numerically to indicate the status of power switches in the order Sa, Sb, Sc. The vector space for stator flux in the stationary reference frame  $\alpha\beta$  is divided into six equal sectors to achieve the circular stator flux trajectory, as shown in Fig.5. The sector is chosen based on the estimated stator flux position, which is calculated using the  $\alpha$  and  $\beta$ -axis stator flux components, as illustrated in (11).

$$\theta = \arctan\left(\frac{\psi_{s\alpha}}{\psi_{s\beta}}\right) \quad (11)$$

Where  $\theta$  represents angle of the stator flux.


 Fig. 5. Sectors and Voltage space vectors in  $\alpha\beta$  reference frame. Source:[9]

Closed-loop torque and stator flux linkage magnitude control is required for classical DTC of PMSM. The stator flux linkage and torque hysteresis comparators are depicted in the proposed DTC control of PMSM as shown in Fig.6 and the logic is shown in (12) and (13).

$$e_\phi = \begin{cases} 1 & (|\psi_s|^* - \psi_s > 0) \\ -1 & (|\psi_s|^* - \psi_s < 0) \end{cases} \quad (12)$$

$$e_\tau = \begin{cases} 1 & (T_e^* - T_e > 0) \\ 0 & (T_e^* - T_e = 0) \\ -1 & (T_e^* - T_e < 0) \end{cases} \quad (13)$$

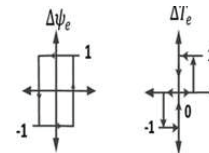


Fig. 6. Hysteresis level

Here  $|\psi_s|^*$  denotes the stator flux linkage reference, and  $e_\phi$  is the stator flux linkage regulator's output. If the value of  $e_\phi$  is 1 indicates that the stator flux linkage needs to be increased, a voltage space vector suitable for the sector will be chosen. Otherwise, the stator flux linkage must be reduced. The torque reference is  $T_e^*$ , and the torque regulator's output is  $e_\tau$ . If the value  $e_\tau$  is 1, the real torque is less than the reference, otherwise it is greater. Table 1 is created by evaluating all the possible combinations of stator flux linkage and torque regulator outputs.

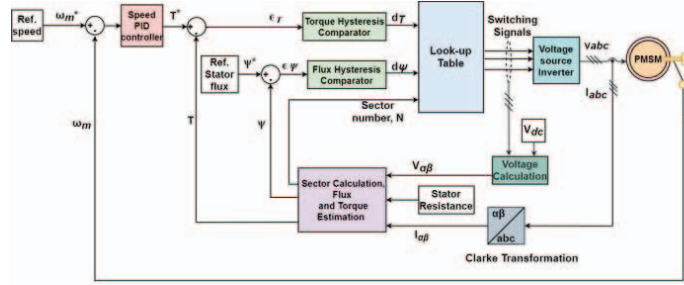


Fig. 7. Block diagram of Direct Torque Control of PMSM

TABLE 1

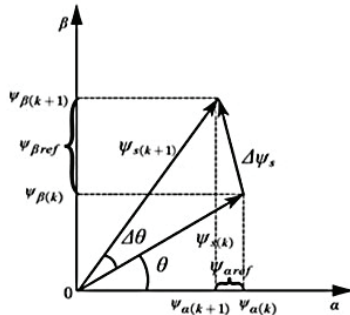
SWITCHING TABLE FOR THE SELECTION OF SPACE VECTORS IN DIFFERENT SECTORS

Sector $\theta(N)$						
$e_\phi$	$e_T$	$\theta(1)$	$\theta(2)$	$\theta(3)$	$\theta(4)$	$\theta(5)$
-1	-1	$V_5$	$V_6$	$V_1$	$V_2$	$V_3$
-1	0	$V_0$	$V_7$	$V_0$	$V_7$	$V_0$
-1	1	$V_3$	$V_4$	$V_5$	$V_6$	$V_1$
1	-1	$V_6$	$V_1$	$V_2$	$V_3$	$V_4$
1	0	$V_7$	$V_0$	$V_7$	$V_0$	$V_7$
1	1	$V_2$	$V_3$	$V_4$	$V_5$	$V_6$

## VI. DIRECT TORQUE CONTROL STATE VECTOR MODULATION (DTC-SVM)

The DTC-SVM uses a switching SVM vector with constant switching frequency. This control scheme eliminates the use of hysteresis controllers. In the DTC-SVM implementation, the generation of gate signals applied to control the inverter switches is based on a predictive controller. Fig.10 depicts the DTC-SVM control mechanism.

The error of torque  $\Delta T_e = (T_e^* - T_{est})$ , the stator flux linkage reference  $\psi_s^*$  serve as input to the predictive controller in addition to actual flux, and stator resistance. The predictive controller then determines the stator voltage reference vector needed in  $\alpha\beta$  frame. coordinates  $V_{sref} = (V_{s\alpha-ref}, V_{s\beta-ref})$  for space vector modulator (SVM), which finally generates the pulses ( $S_a, S_b, S_c$ ) for inverter control. A PID controller that produces the increment of the load angle can minimize the instantaneous torque error. Fig.8 gives an idea on calculating change in flux and flux angle for required torque change in stationary  $\alpha\beta$ - frame.

Fig. 8. Change of flux value in stationary  $\alpha\beta$  frame. Source:[9]

$$\Psi_s = \int (U_s(t) - R_s i_s(t)) dt \quad (14)$$

Through the discretization of (14), it can be shown that:

$$\Psi_{ref} = \Psi_{s(k+1)} - \Psi_{s(k)} = (U_{s(k)} - R_s i_{s(k)}) / T_s \quad (15)$$

## VII. SIMULATION RESULTS

MATLAB/Simulink® R2018b 9.2 version software has been used to implement the models. According to the theory mentioned in the above chapters, various models have been simulated for different speed control schemes. Every simulation is done in a discrete environment with microseconds sampling time. For all the models, the ode45 solver is used to complete the simulation. The simulation focuses on the motoring operation of PMSM in the constant flux region of operation. Some simulations were simulated and executed to get results for the comparison of different control schemes. The machine parameters shown in Table 2 correspond to the non-salient sinusoidal flux distribution 3-phase PMSM motor.

TABLE 2  
PMSM MACHINE PARAMETERS (SIEMENS 1FK7)

Parameters	
Rated Output Power, $P_{out}$	2.135 kW
Rated speed (mechanical), $N_{rated}$	750 rpm
Rated frequency, $f_{rated}$	50 Hz
Rated Torque, $T_{rated}$	6.8 N-m
Rated Current, $i_{rated}$	4.4 A (RMS)
Pole Pairs, $P$	4
Stator Resistance, $R_s$	1.09 $\Omega$
Stator Inductance, $L_{sd}, L_{sq}$	0.009 H
Moment of Inertia, $J$	$4.15 \times 10^{-4}$ kg-m <sup>2</sup>
Damping coefficient, $B$	$1 \times 10^{-4}$ N-m-s/rad
Permanent Magnet Flux, $\psi_{PM}$	0.1821 Wb
Stator Flux reference	0.2 Wb
2-level Voltage Source Inverter (VSI) DC link voltage, $V_{dc}$	400 V

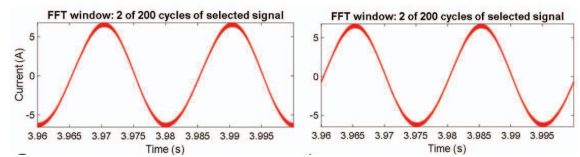


Fig. 9. Steady-state stator phase currents at 750rpm and 6.8 Nm for Open loop SPWM control (left) and Open loop SVPWM control(right)

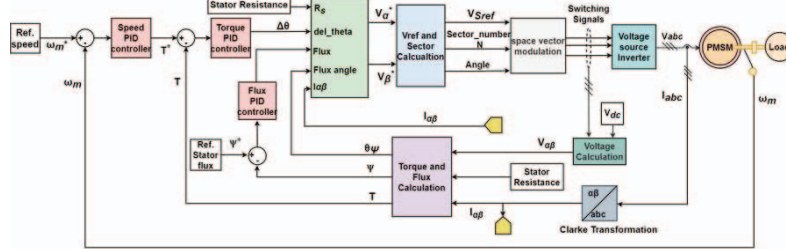


Fig. 10. Block diagram of DTC-SVM of PMSM

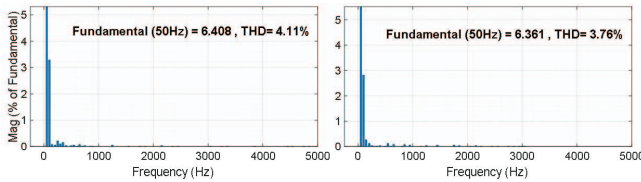


Fig. 11. Harmonic spectrum of steady-state current in Open loop SPWM control (left) and Open loop SVPWM control (right)

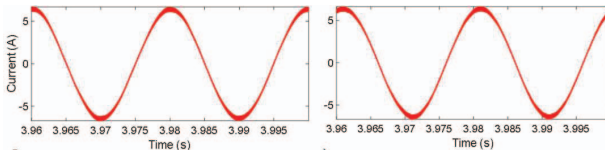


Fig. 12. Steady-state stator phase currents at 750rpm and 6.8 Nm for closed loop SPWM control (left) and closed loop SVPWM control(right)

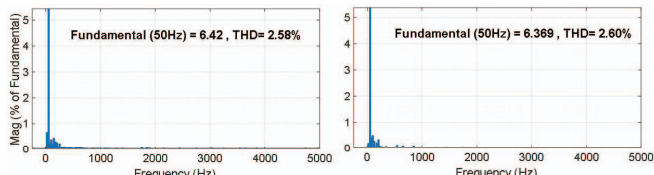


Fig. 13. Harmonic spectrum of steady-state current in closed loop SPWM control (left) and closed loop SVPWM control (right)

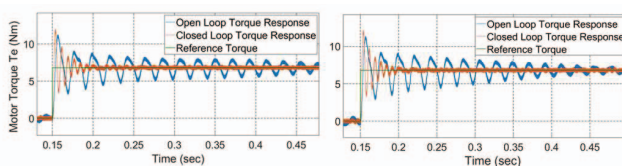


Fig. 14. Torque response comparison of open loop and closed loop using SPWM &amp; SVPWM

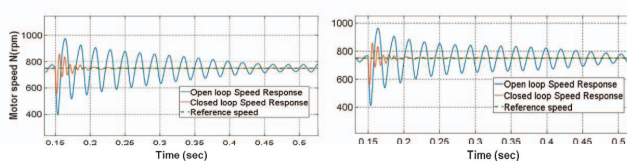


Fig. 15. Speed response comparison of open loop and closed loop using SPWM &amp; SVPWM

TABLE 3

TORQUE FOR SCALAR CONTROL (AT FULL-LOAD TORQUE OF 6.8 N·M AND RATED MECHANICAL SPEED OF 750 RPM)

	Closed-loop SPWM	Closed-loop SVPWM	Open-loop SPWM	Open-loop SVPWM
Steady-state torque ripple (%)	10.848	9.378	15.324	14.563
Torque settling time	90 ms	75 ms	1050 ms	950 ms

From the speed and torque response comparison graph from fig.14 and fig.15, respectively, it is observed that closed-loop control is giving a much better response in terms of steady-state as well as in transient state compared to the open-loop model. At  $t = 0.15$  sec, a rated step load torque of 6.8 Nm is applied. Due to the load torque, a high amount of speed ripple is observed in open-loop control, which has a settling time of around 0.95 sec whereas in closed-loop control speed settles in about 0.14 sec.

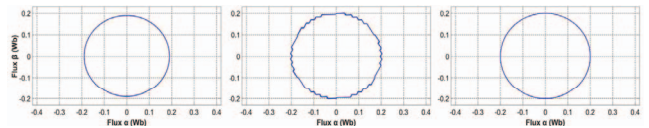


Fig. 16. Steady-state stator flux linkage trajectory for FOC (left), DTC (center) and DTC-SVM (right)

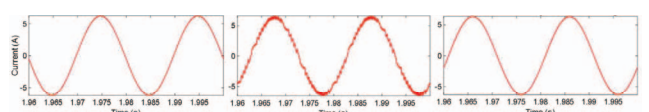


Fig. 17. Steady-state stator phase currents at 750rpm and 6.8 Nm for FOC (left), DTC (center) and DTC-SVM (right)

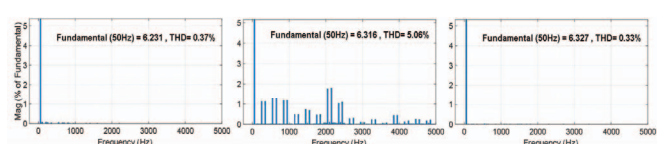


Fig. 18. Harmonic spectrum at 750rpm and 6.8 Nm for FOC (left), DTC (center) and DTC-SVM (right)

TABLE 4

STEADY-STATE PHASE CURRENT THD (%) (AT FULL-LOAD TORQUE OF 6.8 N-M AND RATED MECHANICAL SPEED OF 750 RPM )

THD (%)						
DTC	FOC	DTC-SVM	Closed-loop SPWM	Closed-loop SVM	Open-loop SPWM	Open-loop SVM
5.07	0.37	0.33	2.58	2.60	4.11	3.76

TABLE 5

STEADY-STATE STATOR FLUX RIPPLE (%) (AT FULL-LOAD TORQUE OF 6.8 N-M AND RATED MECHANICAL SPEED OF 750 RPM )

Steady-state stator flux ripple (%)						
DTC	FOC	DTC-SVM	Closed-loop SPWM	Closed-loop SVM	Open-loop SPWM	Open-loop SVM
4.15	0.48	0.36	1.78	1.78	1.79	1.79

Steady-state stator phase current is shown in fig.9, fig.12, fig.17 for open-loop, closed-loop scalar control and vector control, respectively. Table 4 shows the current THD (%) at rated operation for all the control schemes implemented, which is observed from fig.11, fig.13, fig.18. It is evident that DTC suffers from high distortion. DTC-SVM offers the lowest THD (%), closely followed by FOC. Fig.16 shows the steady state stator flux linkage for vector controls. The steady state stator flux ripple (%) from table 5 is maximum in the case of DTC. The steady state flux ripple among scalar control is nearly the same, irrespective of closed-loop or open-loop. The flux ripple is minimum at DTC-SVM. The speed and torque responses at rated load torque for vector control schemes implemented is shown at 100 rpm, 400 rpm and 750 rpm mechanical speed. Fig.19-Fig.21

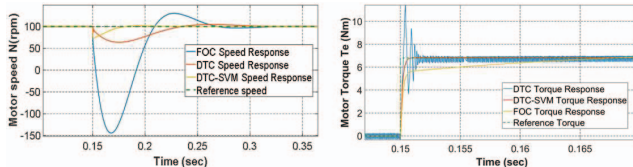


Fig. 19. Speed and Torque Response of Vector Control at 100 rpm left & right respectively for a step load torque change

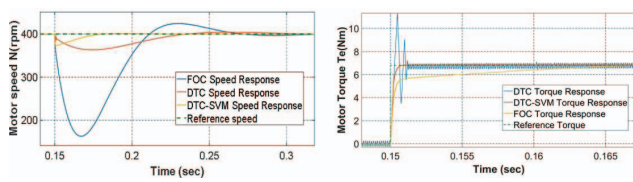


Fig. 20. Speed and Torque Response of Vector Control at 400 rpm left & right respectively

TABLE 6

TORQUE SETTLING TIME AT DIFFERENT SPEEDS ( FULL-LOAD TORQUE OF 6.8 N-M )

Mechanical Speed	DTC	FOC	DTC-SVM
100 rpm	30 ms	139 ms	40 ms
400 rpm	35 ms	143 ms	43 ms
750 rpm	40 ms	150 ms	50 ms

TABLE 7

STEADY-STATE TORQUE RIPPLE (%) (AT FULL-LOAD TORQUE OF 6.8 N-M )

Mechanical Speed	DTC	FOC	DTC-SVM
100 rpm	10.03	1.20	1.15
400 rpm	7.89	1.37	1.36
750 rpm	6.84	1.50	1.57

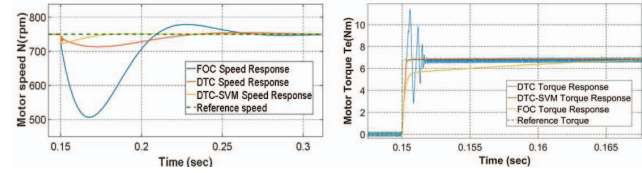


Fig. 21. Speed and Torque Response of Vector Control at 750 rpm left & right respectively

Table 6 shows the torque settling time at speeds of 100rpm, 400 rpm and 750 rpm for rated torque of 6.8 N-m for the different vector control schemes. It is observed that for a particular load, for each control scheme, torque settling time increases as speed reference increases. Also, it is shown that DTC and DTC-SVM offer a faster dynamic response as compared with FOC. Table 7 shows that the torque ripple (%) is highest in DTC for different reference speeds given. The torque ripple increases with increases in reference speed given for FOC and DTC-SVM. In the case of DTC, torque ripple increases with a decrease in speed. This suggests that DTC shows poor performance at low speed.

Table 8 shows the speed settling times at rated operation and no-load rated speed operation for all the control schemes implemented. It is evident that speed settling time increases as load torque increases. DTC-SVM offers the fastest response. It is observed that Variable frequency drives provide better dynamic performance than constant frequency. Table 9 provides a brief summary of comparison between different vector controls. Scalar control techniques are proper for low-

TABLE 8

SPEED SETTLING TIME AT DIFFERENT LOADS ( AT RATED MECHANICAL SPEED OF 750 RPM )

Load Torque	DTC	FOC	DTC-SVM	Closed-loop SPWM	Closed-loop SVM	Open-loop SPWM	Open-loop SVM
0 Nm	100 ms	135 ms	46 ms	130 ms	120 ms	250 ms	200 ms
6.8 Nm	165 ms	185 ms	72 ms	150 ms	140 ms	1050 ms	950 ms

TABLE 9

OVERVIEW OF THE COMPARISON BETWEEN DTC, FOC AND DTC-SVM

	<b>DTC</b>	<b>FOC</b>	<b>DTC-SVM</b>
<b>Reference frame</b>	Stationary ( $\alpha\beta$ )	Rotor (d, q)	Stationary ( $\alpha\beta$ )
<b>Dynamic response of torque</b>	Fast	Slow	Fast
<b>Steady-state behaviour for stator flux, torque and current</b>	High ripple and distortion	Low ripple and less distortion	Low ripple and least distortion
<b>Rotor position requirement</b>	No	Yes	No
<b>Current control</b>	No	Yes	No
<b>PWM modulator</b>	No	Yes	Yes
<b>Coordinate transformation</b>	No	Yes	No
<b>Switching frequency</b>	Variable, depends on the operating point and during the transients.	Constant	Constant
<b>Sampling frequency</b>	Very high	High	High
<b>Control tuning</b>	Hysteresis bands	PID gains	PID gains
<b>Complexity and Processing requirements</b>	Low	High	Very high
<b>Switching Losses</b>	High	Low	Low

speed changing applications but not appropriate for sensitive speed and torque adjustments needed applications. This is because the V/Hz control method controls the magnitude of stator voltages based on the frequency of operation instead of controlling the phase and magnitude of currents. Vector control enables the elimination of cross-coupling terms by transforming 3-phase quantities into orthogonal 2-phase quantities for precise control and hence faster responses and satisfies the requirements of dynamic drives, where quick response is desired. Compared to scalar control, the advantages of vector control are better torque response, producing full load torque at close to zero speed and near-perfect speed control. However, complexity and cost is the trade-off. It is a high-performance control.

Only if the mean switching frequency of inverter operation is approximately comparable for all control schemes can a fair comparison be conducted. Classic DTC, on the other hand, has a variable switching frequency due to hysteresis blocks, which is depending on the operating point of the system.

### VIII. CONCLUSION

The market for PMSM has resulted from the motor requirements such as reliability, good performance, low power loss, simple, cheap and low maintenance requirements. This research develops and implements VSI-fed PMSM in MATLAB/Simulink. The standard scalar (constant V/f) control is used for sinusoidal PWM and space vector PWM for PMSM and has been found to lead to high adjustment and low dynamic response time even though the control is cheap and basic. The vector controls (DTC, DTC-SVM, FOC) of

PMSM had been increased and applied. DTC is used to manage torque and flux efficiently with no variations in machine parameters and load value. The speed and torque can be regulated directly by a DTC inverter vector. DTC can be used in PMSM for a variable speed application. Applications requiring good dynamic efficiency need DTC because it has a greater benefit than other control methods due to its fast torque response characteristics. The findings of the simulation were analyzed and find that the motor torque has more ripple and high THD percent in motor current. Thus FOC control is examined to minimize the ripple content, which has dramatically improved the THD percent, but has exacerbated the machine's complex response. It is introduced with a predictive controller to maintain rapid volatile and low ripple material with constant DTC-SVM frequencies. The results were obtained to promote the tests on broader structures of the proposed approaches.

### REFERENCES

- [1] I. Boldea, A. Moldovan and L. Tutelea, "Scalar V/f and I-f control of AC motor drives: An overview," 2015 Intl Aegean Conference on Electrical Machines & Power Electronics (ACEMP), 2015 Intl Conference on Optimization of Electrical Electronic Equipment (OPTIM) & 2015 Intl Symposium on Advanced Electromechanical Motion Systems (ELECTROMOTION), 2015, pp. 8-17, doi: 10.1109/OPTIM.2015.7426739.
- [2] C. Ed-dahmani, H. Mahmoudi, and M. Elazzaoui, "Direct torque control of permanent magnet synchronous motors in MATLAB/SIMULINK," presented at the 2016 2nd International Conference on Electrical and Information Technologies (ICEIT), May 2016. doi: 10.1109/eitech.2016.7519641.
- [3] Zhuqiang Lu, Honggang Sheng, H. L. Hess and K. M. Buck, "The modeling and simulation of a permanent magnet synchronous motor with direct torque control based on Matlab/Simulink," IEEE International Conference on Electric Machines and Drives, 2005., 2005, pp. 7 pp.-1156, doi: 10.1109/IEMDC.2005.195866.
- [4] Chen Ming, Gao Hanbing, and Song Hongming, "Simulation study on a DTC system of PMSM," presented at the 2011 6th International Forum on Strategic Technology (IFOST), Aug. 2011. doi: 10.1109/ifost.2011.6021087.
- [5] Y. Liu, "Space Vector Modulated Direct Torque Control for PMSM," in Advances in Computer Science, Intelligent System and Environment, Springer Berlin Heidelberg, 2011, pp. 225–230.
- [6] E. Yesilbag and L. T. Ergene, "Field oriented control of permanent magnet synchronous motors used in washers," 2014 16th International Power Electronics and Motion Control Conference and Exposition, 2014, pp. 1259-1264, doi: 10.1109/EPEPEMC.2014.6980685.
- [7] Garcia, X.D., Zigmund, B., Terlizzi, A.A., Pavlanin, R., & Salvatore, L. (2011). Comparison between FOC and DTC Strategies for Permanent Magnet Synchronous Motors. *Advances in Electrical and Electronic Engineering*, 5, 76-81.
- [8] Ö. Türksoy, Ü. Yilmaz, A. Tan, and A. Teke, "A Comparison Study of Sinusoidal PWM and Space Vector PWM Techniques for Voltage Source Inverter," *Natural and Engineering Sciences*, vol. 2, no. 2, pp. 73–84, Jun. 2017, doi: 10.28978/nesciences.330584.
- [9] Cai, Junxi, "Implementation and Analysis of Direct Torque Control for Permanent Magnet Synchronous Motor Using Gallium Nitride based Inverter" (2018). Electronic Theses and Dissertations. 7502. <https://scholar.uwindsor.ca/etd/7502>
- [10] L. Zhong, M. F. Rahman, W. Y. Hu and K. W. Lim, "Analysis of direct torque control in permanent magnet synchronous motor drives," in *IEEE Transactions on Power Electronics*, vol. 12, no. 3, pp. 528-536, May 1997, doi: 10.1109/63.575680.